NIKHEF

NATIONAAL INSTITUUT VOOR KERNFYSICA EN HOGE-ENERGIEFYSICA

November 1983 NIKHEF-H/83-19

THE CONSTRUCTION AND PERFORMANCE OF LARGE MWPC'S FOR THE EXPERIMENT NA11

C. Daum, H. Dijkstra, C. Hardwick,
W. Hoogland, G. de Rijk, H. Tiecke and L. Wiggers
NIKHEF-H, Amsterdam, The Netherlands

NIKHEF SECTIE H POSTBUS 41882, 1009 DB AMSTERDAM

1. INTRODUCTION

A system of large planar proportional chambers has been built in the Mechanical Workshop of NIKHEF-H, Amsterdam. The chambers were used to provide coordinate data for on-line track reconstruction using the FAMP system in the NA11 experiment at CERN. The system was first used as an effective mass trigger for a high statistics inclusive ϕ experiment.

In this report we describe the design, construction and performance of the chambers, with its associated read-out system.

2. DESIGN REQUIREMENTS

A schematic view of the NA11 spectrometer is shown in Fig. 1.

Our trigger requires the presence of two oppositely charged kaons after the 2 magnets of the spectrometer. The signature for a kaon is a signal in an element of the hodoscope MA or MB and no light in the corresponding mirror of the Cerenkov counter C2 or C3 respectively.

The sensitivity of the experiment can be increased by an order of magnitude if the momentum of the two kaons is determined on-line. Therefore we decided to equip the spectrometer with 5 MWPC-planes. The chambers had an active area of (3.84×0.94)m. In the experiment there were two double modules, each with sense wires of $\pm 7.125°$ inclination and one single module with vertical (0°) wires.

The double module proportional chambers P31 and P32 were placed either side of the C2 Cerenkov counter, P32 being placed immediately behind the MA array, allowing an easy correlation between the wires hit and the scintillator elements. The single module P33 was placed about 2 m downstream of P32.

The FAMP system used the independent view of the double modules to calculate the momentum of tracks consistent with the scintillator Cerenkov elements

contributing to the trigger. The application of the FAMP to the on-line event selection is described in more detail elsewhere[1]. Real tracks would have the same momentum calculated from both views. The 3rd chamber provided an extra point on the track in an independent projection to remove ghosts. Tracks with momenta outside the kaon windows of the Cerenkovs were rejected.

Monte Carlo simulations showed that the granularity of the chambers required to achieve the desired momentum resolution was 2 mm, 4 mm and 8 mm for P31, P32 and P33 respectively, while keeping the amount of read-out electronics minimal.

The active area of the chambers had to match the size of the mirrors of C2 so that no acceptance losses would be introduced. An active area of (3.84×0.94) m was chosen. In order to make the construction standardized and allow for interchangeability of modules, all chambers were made with the same dimensions and with 2 mm sense wire spacing. The desired granularity was obtained by OR-ing together 2 and 4 wires for the P32 and P33 modules, respectively.

In order to desensitize the beam region four different areas, which could be held at a reduced cathode voltage, were required on the cathode planes (dead areas). Several areas were required due to the different energies, divergences and polarities of the beam and the different positions of the modules along the beam. Again, in order to standardize construction and allow interchangeability of modules, these areas were made of the same dimensions for each chamber.

3. CONSTRUCTION

3.1 Introduction

The chambers were constructed as a sandwich of several different, rectangular, vetronite frames. For a single module there were 2 gas foil frames, 2 graphite coated mylar cathode frames, a spacer frame, and a wire (20 μm goldplated tungsten) anode frame. The double module had an extra wire plane and an extra cathode plane as a common cathode foil for both wire planes.

The different chamber frames were constructed out of 2 layers of 3.3 mm vetronite, glued together. This determined the gap between the wires and cathode to be 6.6 mm. The various frames were assembled together and held in place by M6 bolts, tightened to a torque of 3 kg.m. The alignment of the frames with respect to each other was kept by precision dowels at each corner. A cross-section of a double module is shown in Fig. 2. A fully assembled module is shown in Plate 1.

External pointers were attached to the wire planes after assembly to 3 dowels in the upper horizontal span of the chamber, so that alignment in the experiment could be achieved. The chambers were suspended from support beams which were on the NA11 rail system.

The wire and cathode frames were prestressed so that no bulky support structures were required in order to maintain the wire and foil tensions respectively. This enabled the P32 module to be placed as close as possible to the MA array. Furthermore the prestressing technique ensured a light construction which made it possible to service the chambers with 2 people without the need for a crane.

It was decided to use graphite coated mylar foils as cathode planes allowing the possibility of separate graphite patches for cathode read-out to be made at a later date. Graphite foils enable the construction of the dead areas to be simple compared to dead areas made with wire cathodes. Technically, foils are also cheaper, simpler, and quicker to construct than wires planes. The continuous equipotential surface of foils results in a higher field at the anode than for wire cathodes at the same voltage.

In order to prevent gas pressure from distorting the frames too much and hence reducing the foil and wire tension, the 3 mm vetronite gas foil frame was stiffened by adding sheet steel of thickness 0.5 mm to each side (7,8 in Fig. 2), riveting steel "L" profiles (13 in Fig. 2) to the outside and using steel gas inlet/outlet pipes (11,12 in Fig. 2).

The gas foils were made from 50 μm mylar/15 μm Al for gas tightness and water vapour impermeability respectively. The Al foil also screens the anode wires from high frequency noise.

In the following we discuss the construction and mechanical tolerances in more detail. In considering the tolerances, we wanted a uniformity of operation over the active area of the chamber to ±100 V.

3.2 Cathode Foils and Gap Separation

The mylar was stretched to a tension of 350 N/m on a large metal frame. The vetronite frame was prestressed with 3 bars connected across the shortest span, tightened to a tension which could create the same deformation of the frame as the tension in the mylar[2] (Fig. 3). The mylar foil was then placed on top of the vetronite and glued along a 2.5 cm band along the inner edge of the vetronite with silicon kit glue[a]. The glue was allowed to set for 24 hours before the prestress bars were removed and the mylar cut to size.

When voltage is applied between the anode wires and the cathode foils, the cathode foils are deflected inwards. The deflection dz is given by:

$$dz = ph^2/T, \tag{1}$$

where T is the tension of the foil, h is half the length of the foil, P is the pressure on the gas foil given by:

$$p = \frac{c^2 \cdot V^2}{8 \cdot \varepsilon_0 \cdot s^2} \tag{2}$$

where c is the capacitance / unit length of the wire, V the high voltage, s the wire spacing and ε_0 the dielectric constant for the vacuum.

---

a) Silicon kit glue, Perpekta Chemie, Goes, The Netherlands.

To keep the voltage variation to 1% requires dz/z good to 1%, i.e. a dz of about 1/10 mm. From 1 and 2 this would result in too high a tension in the mylar. Therefore 2 spacers (garlands and a field restoring wire) were placed horizontally between the wire and the cathode. This reduces the length of displacable foil by a factor 3, and hence the deflection by a factor 9. With a tension of 350 N, h=0.157 m, s=2 mm, and C=4.23 pF/m,

$$dz = 4.4\ V^2\ \mu m$$

which is 0.11 mm at 5 kV.

For the double modules there is no electrostatic displacement of the common central foil.

3.3 Garlands and Field Restoring Wire

The garlands were made from 5.75 mm wide, 0.05 mm thick Kapton foil. The foil was made into a zigzag shape and stretched across the chamber together with an insulated wire of diameter 0.85 mm, which together have a thickness of 6.6 mm, the chamber gap thickness. The garland was supported on a nylon thread which passed through holes punched in the garland. The field restoring wire (FRW) was attached to this thread with small pieces of silk thread at various places. The nylon support thread was kept in position by silk thread attaching it to the chamber frame (see Fig. 4 and plate 2). This technique was first used at CERN by Majewski and Sauli[3].

Two garlands were installed for each cathode foil. For each plane the garlands on opposite sides of the sense wire plane were displaced vertically from each other by 3 cm to minimize localized inefficiencies.

3.4 Wire Frames

The wire frames had 1 layer of vetronite removed from the 2-ply sandwich at the upper and lower long spans and replaced with printed circuit boards

(PCB's), which had solder pads and printed circuit strips to get the signal to the external connectors. Two different sets of PCB had to be made for the different angled wire planes.

Twenty microns Au plated Tungsten wire[b] was wound at a tension of 50 g and at a 2 mm pitch on the winding machine of the NIKHEF-H Workshop. The wires were glued to 4 transfer frames on the machine. The wires were kept in the correct position by precision combs. The chamber frames were prestressed in a similar way to the cathode frames (Fig. 3), so that after removal of the prestress bars the wires would remain at the correct tension. The geometry of the transfer frame could be changed so that different angled wire frames could be made. These frames also allowed the wires to be precisely lowered onto the solder pads of the PCB. At this stage of the procedure, the wires were accurately aligned to the chamber frame and relative to each other to within 50 μm (§3.4.2). The wires were then glued with epoxy[c] to the PCB in between the solder pads and the sensitive area of the frame. After allowing the glue to set, the wires were soldered to the pads on the PCB. Further frames were added until the complete chamber frame was wired. The prestress bars were then removed and a control of tensions was made (§3.4.1).

To reduce the unbalanced electrostatic tension on the outer wires of the plane, two guard wires of 50 μm and 100 μm diameter Cu-Be at tensions of 100 and 200 g respectively were fixed as the last wires at each end.

To provide a test pulse for each sense wire, an insulated wire was glued over the top of the solder pads at the opposite end of the wires to the printed circuit strips. A 6 V pulse in this test wire induced a pulse on every sense wire via capacitative coupling.

---

b) 4% Gold plated Tungsten wire - Highways International, Baarn, The Netherlands.

c) Epoxy glue, Araldite AW106, HV95311, CIBA.

3.4.1 wire tensions

For Tungsten wires of 20 μm diameter, the elastic limit is 65 g. The wire frames were wound at a tension of 50 g. An array of such wires spaced at 2 mm and of length 0.94 m is electrostatically unstable. Alternate wires are displaced to one or other of the cathode foils. However, the garland/FRW assembly divides the effective length by 3 and stability is restored. There is a lower limit for wire tension at which a single loose wire would be displaced towards the cathode but this is about 20 g. The wire tensions were actually controlled to ±10 g using a wire tension measuring device[d]. This device measured the frequency of vibration of the wire in a magnetic field.

The prestressing method was checked in the following way. We selected three areas (Fig. 3); region A, where the prestressers were applied; region B, which lies in between two prestressers and region C at the edge of the frame. In this last region we expect the effect of wrong prestressing to be negligibly small and this region is used as a check for possible effects not related to the prestressing. In every region we measured the tension of a group of wires before and after the prestressers were removed. The differences in tension of these wires on a wire by wire basis is shown in Fig. 5 a,b and c for the regions A, B and C respectively. The tension of the wires in region C does not change on average, it shows a distribution around 0 g, indicating the error on the measurement as expected. The wires in the regions A and B have on average lost 2 g of tension, well within the tolerance. Fig. 6 shows the spread in tension of the wires before (Fig. 6a) and after (Fig. 6b) the removal of the prestressers. All wires have a tension which is well within the required tension window of 20-65 g discussed above.

3.4.2 wire positions

It can be shown that a displaced wire in an array of wires has a change in charge and hence operating voltage of:

---

d) Wire tension meter, type: NE-660, METRIMPEX, Budapest, Hungary

$$dV/V = b.(dz/s)^2$$

and that it induces a change in charge and operating voltage on the neighbouring wire of:

$$dV/V = a.(dx/s)$$

where a=0.18; b=0.22 for chambers built with our gap and wire spacing, s=2mm [4], hence we are very sensitive to displacements in the plane of the frame (x-direction).

Some error in the plane perpendicular to the wire plane (z-direction) occurred when glueing the wires to the PCB but the precision was estimated to be better than 0.2 mm; hence dV/V = 0.2% which at 5 kV is equivalent to a change in voltage of ±10 V.

In principle, the precision of the wires in x was good to ±5 μm, the precision of the teeth of the comb on the winding machine. However, some displacement occurred when transferring the wires to the PCB and during glueing. The displacements were rapidly checked before soldering with a Moiré fringe technique developed at NIKHEF-H[5]. Any wire with a deviation of more than 50 μm was replaced. A histogram of wire displacements is shown in Fig. 7. The FWHM is 30 μm. A displacement of 50 μm gives a change in charge of 0.5% corresponding to a change in operating voltage of ±25 V at 5 kV.

3.5 Dead Areas

The dimensions and shape of the dead areas is shown in Fig. 8. Before spraying the foils with graphite, 2 mm wide masking tape was used to create the dead area patches. The leads to the patches for the dead area control were made by spraying the foil with silver paint[e] (graphite had too high a resistivity over a narrow path of 2 mm). Some problems were encountered with

---

e) Silver paint, Perpekta Chemie, Goes, The Netherlands.

breaks occurring in the silver paint during transport of the chamber. These breaks had to be resprayed otherwise breakdowns between dead and live regions were induced.

In principle we could have dispensed with the silver paint leads for the single sided foils by threading a wire from the back of the foil through a small hole in the dead area region and attaching it with conducting araldite.

3.6 Graphite Foils and Resistivity of Graphite

The mylar foils were fixed vertically in a well ventilated enclosure. A spray gun containing a suspension of graphite in isopropanol[f)] was fixed on a movable trolley about 50 cm from the mylar. The foils were then sprayed at 3 different heights by moving the spray gun across the foil. After the first spraying the foils were polished with tissue paper (Kleenex). This procedure was repeated once more and the foils were polished until the required resistivity and uniformity of resistivity was obtained. The resistivity of the foil was chosen low enough to ensure a small voltage drop at the rates we were expecting but high enough to prevent large currents in the case of breakdown.

High voltage was fed from terminals on the outside of the chamber, to the graphite via aluminium foil. The connection between the foil and graphite was made with silver paint. Sometimes this connection broke during transport of the chamber and conducting araldite would have been a better material to use.

The high voltage resistivity between the different dead area patches and between the dead areas and the main cathode was checked in air to 2 kV before assembly of the chamber. The total resistance from the voltage input to any point of the foil surface was kept to less than 100 kΩ. On average this gives a voltage drop for a current of 100 μA of 5 V maximum.

---

f) Graphite colloidal suspension, Acheson Dag 502, Acheson Colloidon BV, Schiedam, The Netherlands.

The above considerations give an overall plateau variation of:

±25 V due to error in wire position in x,
±10 V due to error in wire position in z,
-55 V max. due to electrostatic displacement of the cathode foil,
+ 5 V max. due to voltage drops across graphite;

giving a variation of +40/-90 V at 5 kV.

In practice the chambers were operated at 4.5 kV and the maximum current was about 20 μA during beam spill, hence the overall variation was below the design value of ±100 V.

To check the gain variation, a Ruthenium source was placed at a fixed distance from the chamber and the high voltage adjusted until a certain current was obtained. The source was then moved to other positions on the active area of the chamber and the voltage adjusted until the same current was obtained. In this way the voltage change required to keep the same gain was found to be ±70 V.

4. HIGH VOLTAGE SYSTEM

Each double module had only one high voltage supply[g], so that in turning on, the voltage either side of the central cathode foil was always equal. The dead area voltage was derived from a 40 MΩ divider from the chamber high voltage supply and was equal to ½ of the chamber high voltage. One separate supply was used for the field restoring wire voltage on all planes.

5. GAS SYSTEM

The chambers were operated using Magic Gas consisting of 75% Argon, 24.5% isobutane and 0.5% Freon (Freon 13B1, CF_3BR). The gas was mixed in a

---

g) Rutherford Laboratory High Voltage Supplies, PAG 344.

CERN standard isobutane rack from 25% isobutane, and 37.5% of both Argon and an Argon/1% Freon mixture. The Argon was bubbled through a methylal $\left((OCH_3)_2CH_2\right)$ bath at 0 °C. Gas flow rates to the chamber were 15ℓ/hr for P31 and P32 and 10ℓ/hr for P33, giving a chamber volume change of once every 12 hours.

6. READ-OUT

The Plessey electronics D16/DR32 system was chosen for read-out of the chambers.

Special features of this system are:

1. An acoustic was delay in the D32 receiver modules, the value of which was specified before manufacture. This dispensed with the need for expensive, bulky cable delay.
2. The system is RMH compatible[6], a system which was already in use in the NA11 experiment.
3. The DR32 receiver module contained fast OR ECL output for adjacent groups of 4 wires read-out. This was used in coincidence with the MA array to improve the first stage trigger rejection.
4. The D16 preamplifier/discriminator was equipped with 2 test inputs allowing odd or even channels to be pulsed independently. For our application an input impedance value of 100 Ω was chosen.

The D16 cards each containing 16 channels were mounted in especially constructed crates placed below the chambers in the experiment on movable trolleys.

The chamber wires were connected to the cards by 70 cm flat cables of 100 Ω impedance, which were screened on one side. Each crate could hold 22 modules. P31 had each wire read out. P32 and P33 had groups of 2 and 4 wires OR'd together respectively, by means of an intermediate printed circuit board which could be plugged directly onto the chamber PCB. Oscillation

problems were only encountered in the P33 module where 4 wires were OR'd together but this was cured by grounding the back plane of the chamber PCB to the chamber frame, and increasing the threshold voltage for the pre-amps.

At the back of each crate was a printed circuit board which provided the low voltage power lines of -5.2 V and ground, a threshold control line, and the two test pulse input lines.

The threshold of the discriminator was controlled in each crate by a potentiometer connected across the threshold control line and ground. This allowed a variation of control voltage from 0.8 to 1.4 V corresponding to 540 to 950 μV of threshold. In practice threshold control voltages of 1.1 V for P31,32 and 1.4 V for P33 were used. Below this, oscillations began to occur. The connection between the D16 cards and the D32 read-out units was made with 50 m long cables, each containing 32 twisted pairs.

The D32 modules were housed in RMH crates via which a strobe of 150 ns was applied. A fast clear pulse could also be sent via the RMH crate. The system configuration is shown in Fig. 9; two branches of 4 and 3 crates were used. The "bypass unit" (BU) allowed the FAMP microprocessor access to the data.

6.1 Low Voltage System

The low voltage on the D16 crates was supplied by switched mode power supplies[h]. Each module could supply 40 amps at 5 V.

Each D16 card had a current dissipation of 800 mA. For the complete system 7 modules were required. Two times three in parallel for the 116 cards of P31 and P32, and one module for the 32 cards of P33. Because of the high current drawn by the cards of P31 and P32, 10 mm^2 cross-section cable was used to connect each ± terminal of each module to the crates to prevent too

---

h) "Delta" modules, Delta Elektronika, Zierikzee, The Netherlands.

high a voltage drop in the cables. The voltage was controlled by a sensor connected to the crates. The D16 crate was equipped with 3 fans to cool the cards.

7. PERFORMANCE

The chambers P31 and P32 with a threshold control voltage of 1.1 V and P33 with a threshold control voltage of 1.4 V were on plateau at 4.45 and 4.5 kV respectively. The field restoring wire voltage plateaued at 1.9 kV. With these settings each plane drew about 20 μA in a beam of 2.10^6/sec. Typical plateau curves for the chambers are shown in Fig. 10 and for the FRW regions in Fig. 11. The efficiencies of the chambers were determined using tracks reconstructed from the packs of drift chambers positioned either side of the MWPC's in the spectrometer (DC3A,B and C in Fig. 1). For determining the FRW efficiency, only tracks within ± 6 mm of the FRW were used.

Each chamber had an overall efficiency of 98%, excluding the dead region allowing a combined efficiency of 90% for a hit in every plane for one particle. The residual inefficiency was due to single dead D16 channels and some remaining inefficiency in the FRW zones. A plot of the FRW zone inefficiency is shown in Fig. 12 for no FRW voltage and for full FRW voltage. With beam particles through the centre of the chamber the efficiency was >99.8%.

Some problems were encountered during operation. These were due to breakdown between the dead areas and the high voltage areas of the foil where a 1.0 kV potential difference over a 2 mm gap occurred. Usually this was due to graphite dust, fibres and sharp edges. No problems with sparks from wires to high voltage foil were encountered.

Some cracks in the silver paint leads to the dead area zones (§3.4.3) forced us to reduce the voltage of the 4 dead areas in one MWPC. Since we then created, apart from the dead areas themselves, an 18 mm wide band of reduced voltage from the dead areas to the top of the chamber, we

investigated the effect on the inefficiency in this area. For comparison we show the efficiency profile across the voltage leads for 2 dead areas at reduced voltage (Fig. 13a) and the efficiency profile across the voltage leads for 4 dead areas also at reduced voltage (Fig. 13b), a band of 16 mm width. Also shown is the profile across a dead area boundary (Fig. 13c).

****

ACKNOWLEDGMENTS

We would like to thank O. Runolfsson and M. Uldry of the NA3 collaboration for information on their manufacture of graphite foils which we copied in the construction of our chambers. Also we are much endebted to the members of the drawing office and Mechanical Workshop of NIKHEF-H, in particular we would like to thank N. de Koning, H. Schuijlenburg, H. Vink and M. Kroezen.

We acknowledge many useful discussions with M. Edwards and M. Jeffs of the Rutherford Laboratory, concerning the Plessey read-out system.

++++++++++++++++++

REFERENCES

1. On-line event selection with the FAMP microprocessor system, C. Daum et al., to be published in Nucl. Instr. and Meth. — Proc. of the 1983 Vienna Wire Chamber Conference.

2. Calculations for prestressing frames of particle detectors and forces applied to frames due to gas foils, H. Dijkstra, ACCMOR report 43, 20-8-'80, internal report.

3. Support lines and beam killers for large size multiwire proportional chambers, S. Majewski and F. Sauli, CERN NP internal report 75-14 (75).

4. Electrostatic problems in multiwire proportional chambers, G. Erskine, Nucl. Instr. and Meth. 105 (1972) 565.

5. A simple technique for measuring with high accuracy relative wire positions in MWPC's, H. Dijkstra et al., Nucl. Instr. and Meth. 188 (1981) 59.

6. A fast and flexible data acquisition system for multiwire proportional chambers and other detectors, J.B. Lindsay et al., Nucl. Instr. and Meth. 156 (1978) 329-333.

Plate Captions

Plate 1: Two assembled modules on a support trolley, under test in the NIKHEF-H Mechanical Workshop.

Plate 2: Picture of a chamber during the mounting of the several layers of cathode and wire planes in the Mechanical Workshop of NIKHEF-H. A cathode foil is shown with two garlands. In the centre of the chamber one can distinguish the beam killer patches.

Figure Captions

Fig. 1. Top view of the NA11 spectrometer. MNP33,BBC: magnets; DC2, DC3a,DC3b and DC3c: drift chambers; C1,C2 and C3: Cerenkov counter hodoscopes; MA and MB: scintillation counter hodoscopes; P31ab, P32ab and P33 are the proportional chambers.

Fig. 2. Cross-section of a double module (±7.125°). 1,2: wire frames; 3,4 and 5: cathode frames; 6: spacer frame; 7,8: gas foil frame sandwiched between 0.5 mm steel sheets; 9: distance piece and precision bolt; 10: neoprene O-ring for gas tightness; 11,12: steel gas pipes; 13: steel corner pieces for reinforcement.

Fig. 3. Prestress bars on vetronite frame. A, B and C are the positions where wire tensions were measured to check the prestressing, the result of which is discussed in §3.4.1.

Fig. 4. Exploded view of a garland and an FRW.

Fig. 5. Differences in wire tensions (ΔT) before and after the prestress bars were removed. The tension change of the wires in regions A, B and C (Fig. 3) is shown in Fig. 5a,b and c respectively.

Fig. 6. The tension spread of wires before (a) and after (b) the prestress bars were removed.

Fig. 7. Distributions of wire displacements (Δd) from the ideal position, in the plane of the wire frame, perpendicular to the wires (x-direction).

Fig. 8: Dead area patches viewed along the beam direction. The black lines represent the 2 mm wide separation between the different areas. These lines were taped off during the spraying of the foils with

graphite and the spraying of the dead area voltage leads with silver paint.

Fig. 9. Configuration of the read-out electronics of the proportional chambers.

Fig. 10. Typical plateau curves of 3 out of the 5 planes in the experiment. The efficiency has been determined by requiring a track to be seen in the drift chambers, either side of the MWPC.
The operating voltage for P31 and P32 was 4.45 kV, and for P33 was 4.5 kV. The solid lines are drawn to guide the eye.

Fig. 11. Plateau curves for 2 field restoring wire regions. The operating voltage was chosen to be 1.9 kV. The solid lines are drawn to guide the eye.

Fig. 12. The inefficiency in a vertical projection across 2 field restoring wires. Applying no voltage (solid line) to the FRW shows 2 peaks displaced by 3 cm, the vertical displacement of 2 garlands on opposite sides of the sense wires. The dashed line shows the inefficiency of the FRW region when the FRW was 1.9 kV.

Fig. 13. The inefficiency profile across HV leads for 2 dead areas at reduced voltage a) (inset shows the configuration of the dead area leads); the inefficiency profile across HV leads for all 4 dead areas at reduced voltage b); the inefficiency profile across a dead area boundary c).

* * *

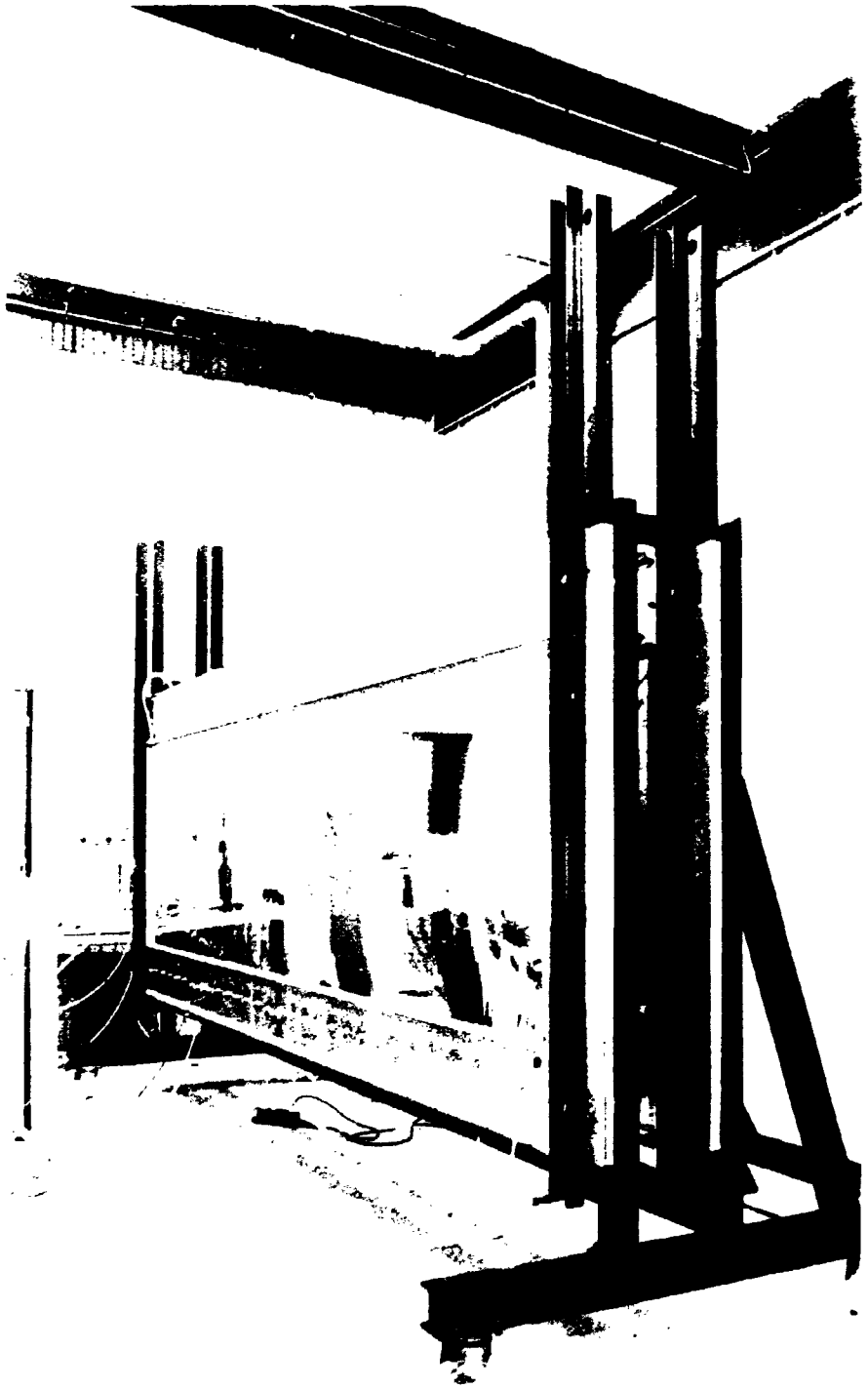

Plate 1.

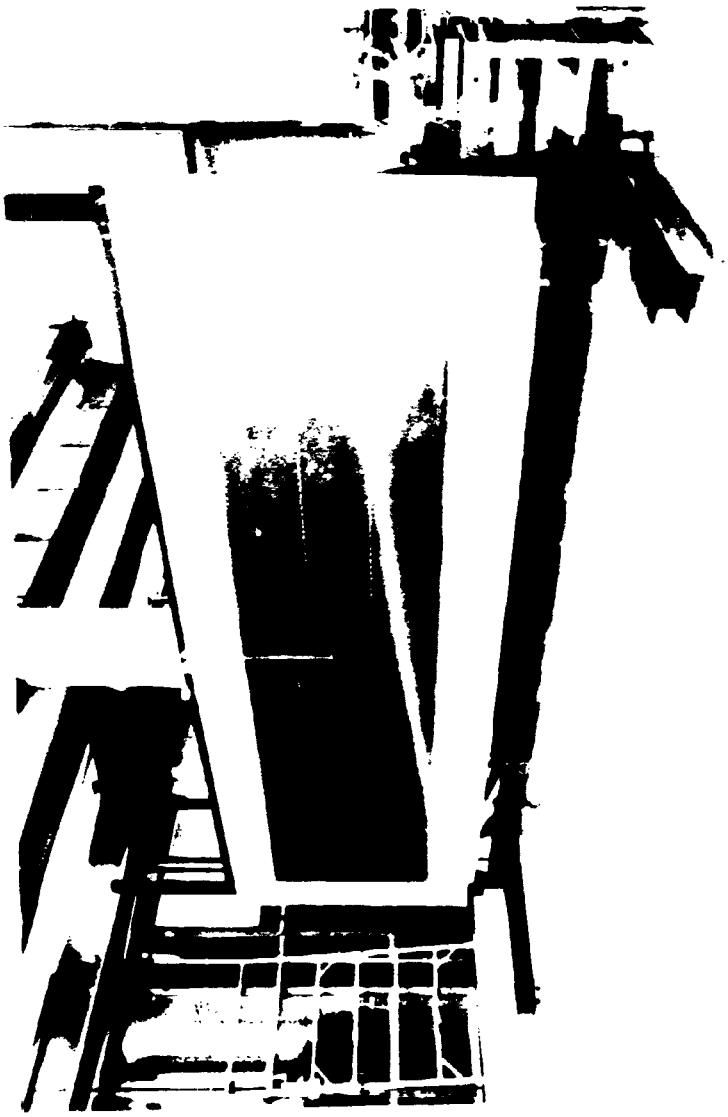

Plate 2.

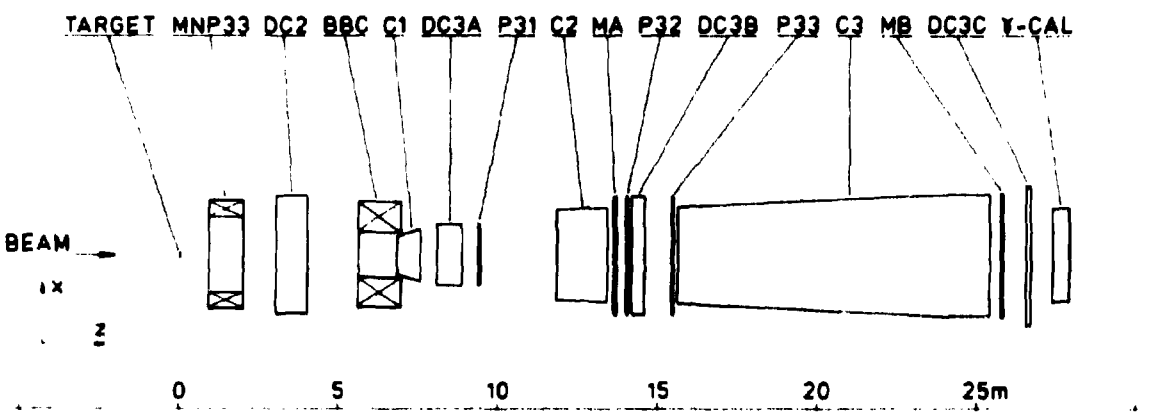
TARGET
MNP33
DC2
BBC
C1
DC3A
P31
C2
MA
P32
DC3B
P33
C3
MB
DC3C
Y-CAL
BEAM
Y
X
Z
0
5
10
15
20
25m

Fig. 1

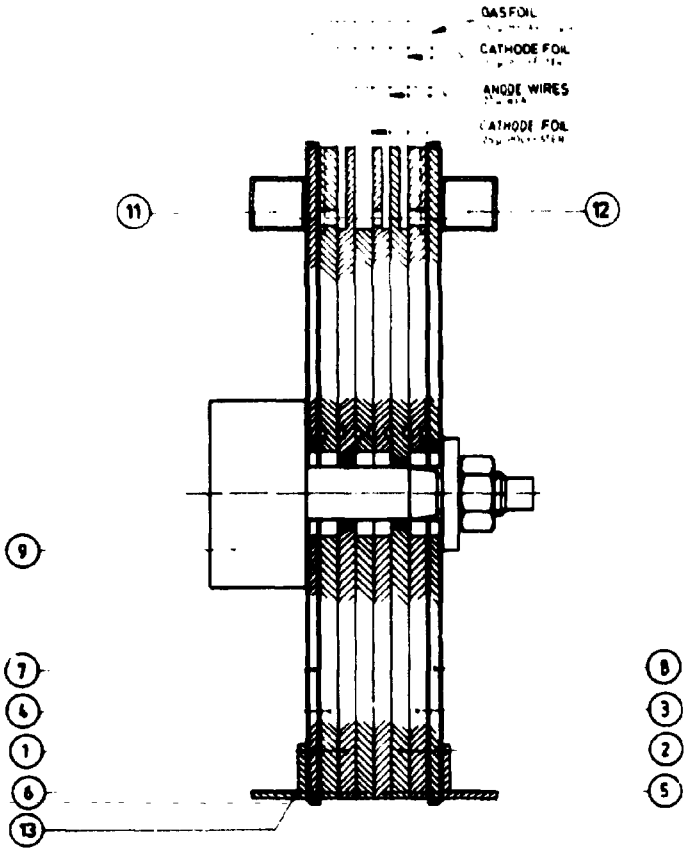

Fig 2

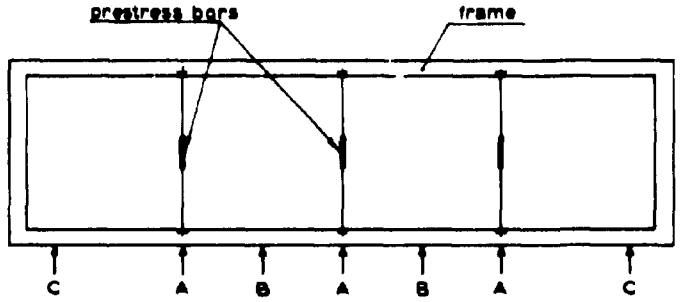

Fig. 3

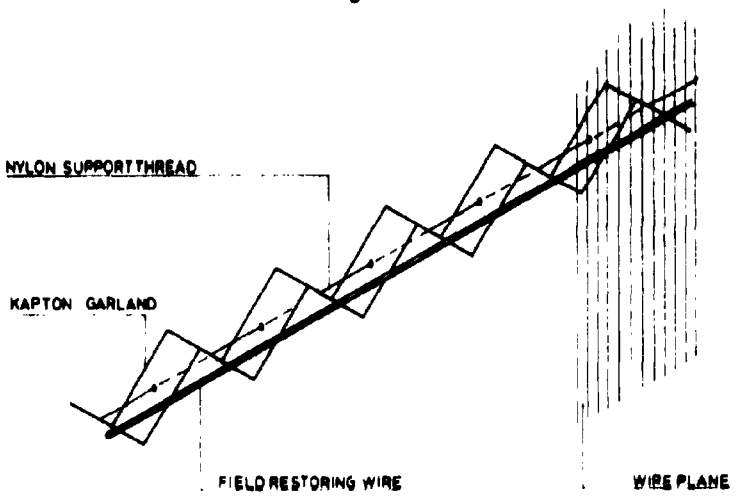

fig 4

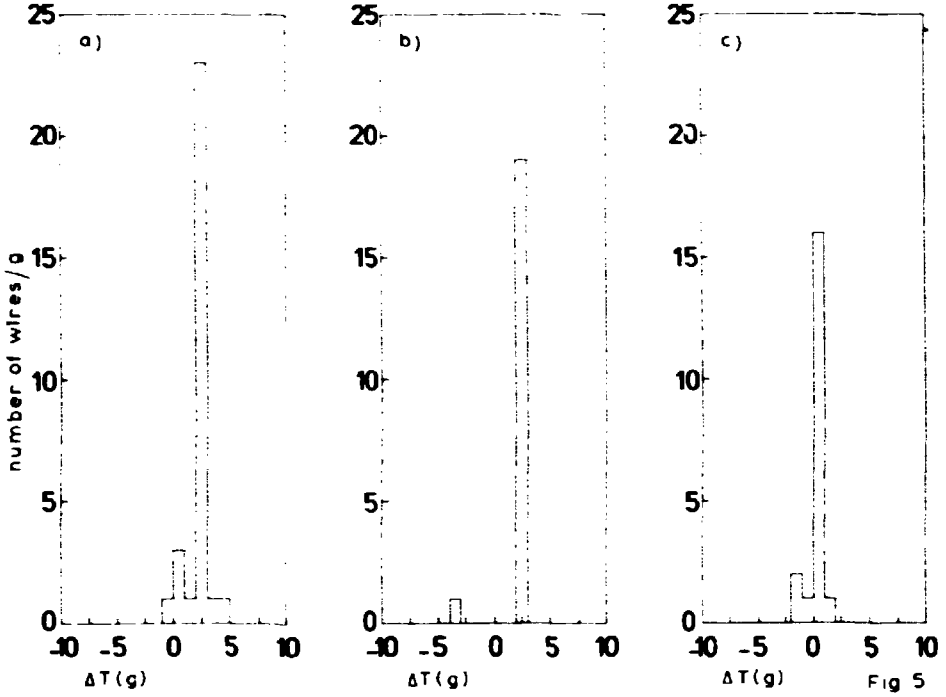
a)
b)
c)
number of wires/g
ΔT(g)
ΔT(g)
ΔT(g)

Fig 5

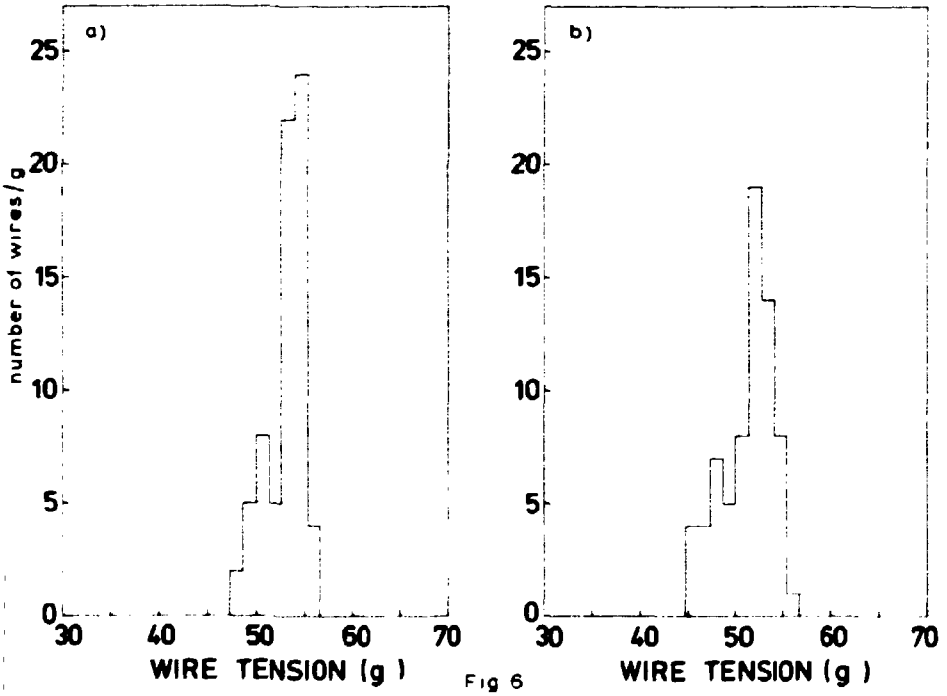
a)
b)
number of wires/g
WIRE TENSION (g)
WIRE TENSION (g)

Fig 6

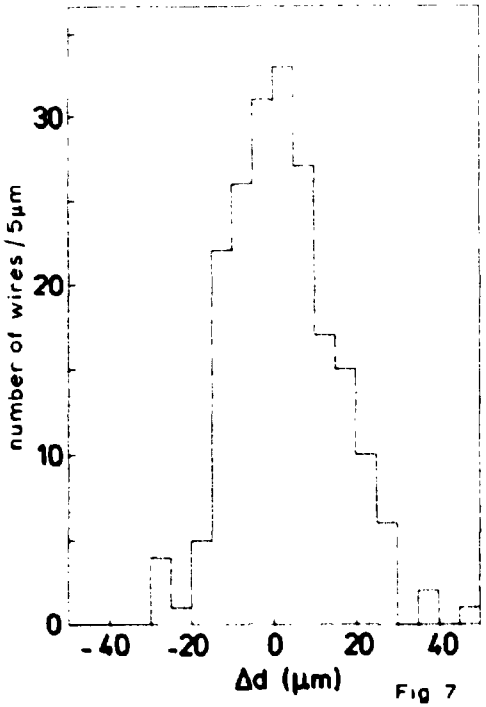

Fig 7

Fig. 8

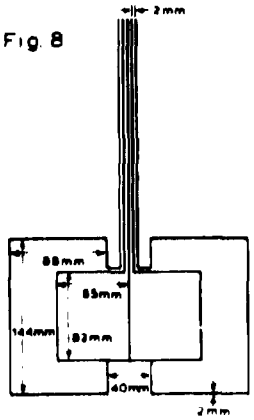

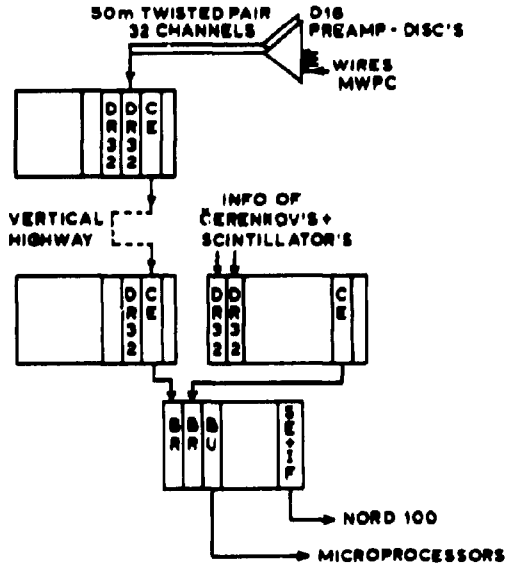

Fig. 9

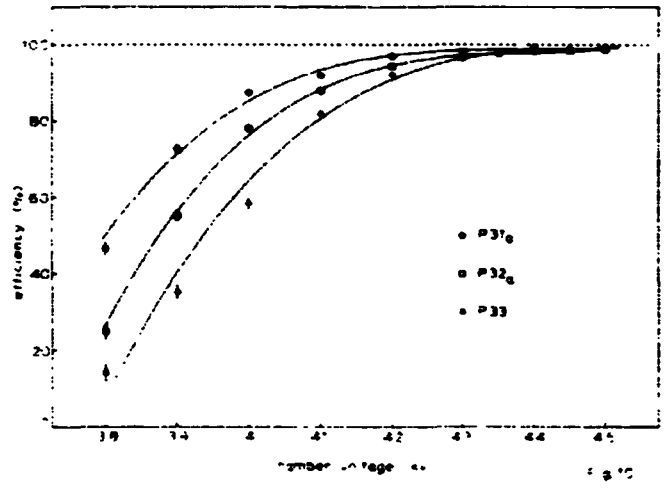
100
80
60
40
20
efficiency (%)
P31
P32
P33
38
39
40
41
42
43
44
45

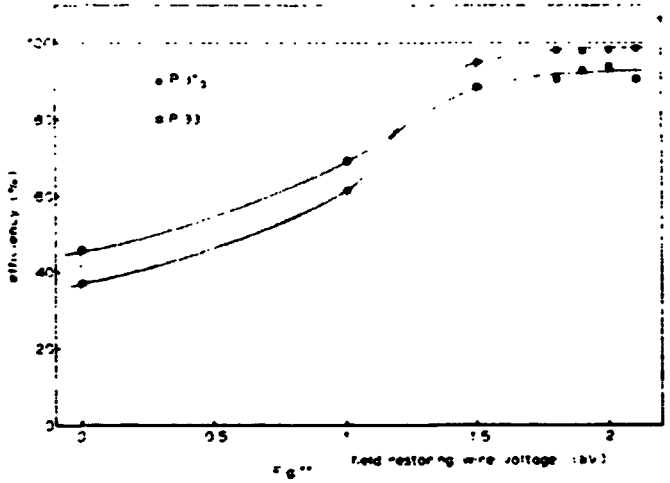
100
80
60
40
20
0
0.5
1
1.5
2
P33

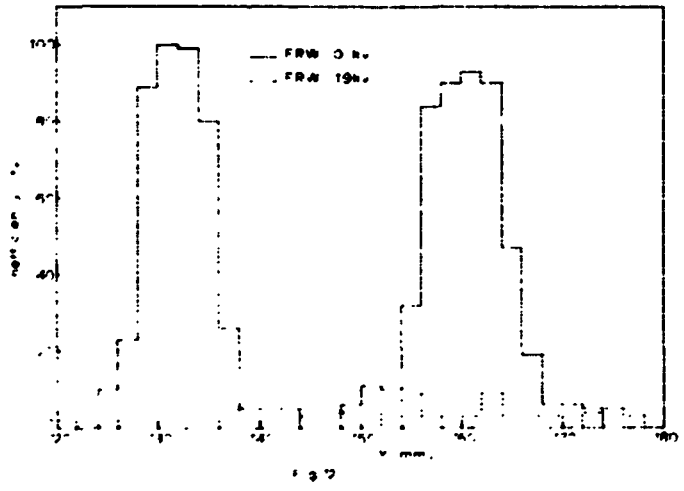
FRW 0 kv
FRW 19kv

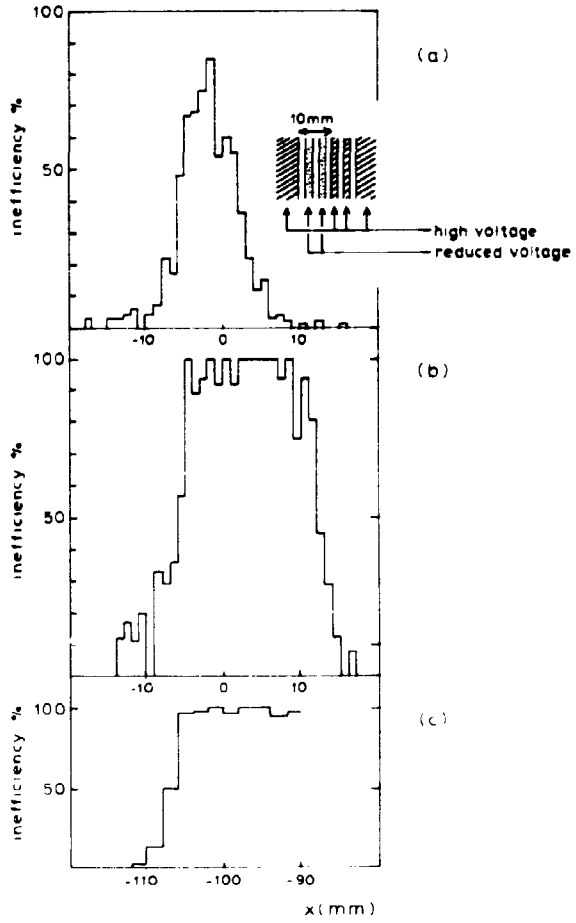
100
50
inefficiency %
(a)
10mm
high voltage
reduced voltage
-10
0
10
100
50
inefficiency %
(b)
-10
0
10
100
50
inefficiency %
(c)
-110
-100
-90
x(mm)

Fig 13